ASCAT Wind Quality Control Near Rain

Wenming Lin, Marcos Portabella, Ad Stoffelen, Anton Verhoef, and Antonio Turiel

***Abstract*—In this paper, anomalous spatial gradients are investigated by an image processing method, known as singularity analysis, which is proposed to complement the current Advanced Scatterometer (ASCAT) quality control (QC) by using the singularity exponent (SE). The quality of ASCAT winds is known to be generally degraded, with increasing values of the inversion residual or maximum-likelihood estimator (MLE). In the current ASCAT Wind Data Processor (AWDP), an MLE-based QC is adopted to filter poor-quality winds, which has proven to be effective in screening artifacts in the ASCAT winds, associated with increased subcell wind variability and other phenomena such as confused sea state. However, some poorly verifying winds, which appear in areas with moist convection, are not screened by the operational QC. The extension of the QC procedure with SEs is investigated, based on a comprehensive analysis of quality-sensitive parameters, using the European Centre for Medium-range Weather Forecasts (ECMWF) model winds, the Tropical Rainfall Measuring Mission's (TRMM) Microwave Imager (TMI) rain data, and tropical buoy wind and precipitation data as reference, taking into account their spatial and temporal representation. The validation results show that the proposed method indeed effectively removes ASCAT winds in spatially variable conditions. It filters three times as many wind vectors as the operational QC, while preserving verification statistics with local buoys. We find that not the rain itself, but the extreme local wind variability associated with rain appears to generally decrease the consistency between ASCAT, buoy, and ECMWF winds.**

***Index Terms*—Quality control (QC), rain, scatterometer, singularity analysis (SA), wind, wind variability.**

I. Introduction

SPACEBORNE scatterometers are known to provide accurate mesoscale 10-m equivalent-neutral wind speed and direction. The wind field inferred from scatterometer measurements is used in a variety of applications, including Numerical Weather Prediction (NWP), nowcasting, climate, and air–sea interaction modeling. The wind retrieval procedure is carried out by inverting the nonlinear relationship between the averaged radar backscatter cross-sections (σ^0) and the mean sea-surface wind vector in a Wind Vector Cell (WVC). However, geophysical phenomena other than WVC-mean wind, such as rain, sub-WVC wind variability, confused sea state, and land/ice contamination within the radar footprint, may also significantly contribute to the backscatter signal measured by scatterometers and, in turn, distort the mean wind-induced signal, leading to poor-quality retrieved winds. Elimination of poor-quality winds and assessing their effect is the prerequisite for using scatterometer data in the already mentioned applications.

Over the last decade, broad studies have sought to better understand the physics of poor-quality scatterometer winds. Particularly, various methods have been developed to address the rain effects on Ku-band scatterometer systems, as categorized by the following three methodologies: filtering rain-contaminated WVCs [1]–[3]; correcting the rain-induced backscatter contribution before wind retrieval by assessing the rain effects on scatterometer backscatter measurements [4], [5]; and modeling both wind- and rain-induced backscatter, with the objective of retrieving wind and rain parameters simultaneously [6], [7]. In case of the C-band ASCAT, an inversion residual or maximum-likelihood estimator (MLE)-based approach is used to flag the poor-quality wind [8]. Operationally, any WVC with MLE $> +18.6$ is flagged as poor wind quality in the current version of AWDP. Although this kind of quality control (QC) has been proven to be effective in rejecting WVCs with poor wind quality, many rain-contaminated measurements, which validate poorly, are not rejected [9]. At low winds, rain may cause enhanced spatial variability, and techniques using spatial derivatives may be complementary in QC of rain cases. Therefore, an image processing technique, known as singularity analysis (SA), has been proposed as a complementary ASCAT QC tool in [9].

SA provides quantitative information about the local regularity or irregularity of an image. Preliminary results in [9] and [10] show the potential of SA to detect not only existing geophysical structures, characterized as singularity fronts, but also any transition due to the presence of retrieval errors. More recently, the SA method has been further developed for the optimization of ASCAT rain identification [11]. It turns out that SA is sensitive to increased inter-WVC wind variability at very local scales (mostly within the nearest neighbor WVCs), generally associated with rain events and frontal structures. Due to the large spatial variability of rain, SA is proven to be more effective than MLE, in terms of exploiting the rain signatures present in ASCAT parameters, particularly for the lower rain rate and low wind conditions, where the MLE is less sensitive to these cases. As a result, SA detects rainy WVCs when the MLE-based QC does not (mostly low rain rates), and MLE detects rainy WVCs when SA does not (mostly high rain rates), indicating that these two techniques are very complementary for the purposes of both rain detection and QC.

Manuscript received April 30, 2014; revised September 2, 2014 and November 4, 2014; accepted December 28, 2014. This work was supported in part by the European Organisation for the Exploitation of Meteorological Satellites Ocean and Sea Ice Satellite Application Facility Associated Scientist Project under Reference OSI-AVS-12-04 and in part by the Spanish Ministry of Science and Innovation (MICINN) National R&D project under Reference AYA2012-39356-C05-03.

W. Lin, M. Portabella, and A. Turiel are with the Institut de Ciències del Mar (ICM–CSIC), 08003 Barcelona, Spain (e-mail: wenminglin@icm.csic.es).

A. Stoffelen and A. Verhoef are with the Royal Netherlands Meteorological Institute (KNMI), 3730 AE De Bilt, The Netherlands.

Digital Object Identifier 10.1109/TGRS.2015.2392372

Using spatial derivatives is however potentially detrimental, as steep wind gradients may be removed, while particularly relevant for some applications. This poses a challenge in verification of the QC scheme as spatial and temporal representativeness are dominating the quality indexes. Moreover, where rain is spatially erratic, it induces downbursts of wind on the ocean surface with strong gust fronts, and as such, rain is associated with enhanced wind variability. Wind verification of a QC scheme by buoy data thus may be penalizing conditions with such high wind variability, since the wind vector measured at a buoy location is generally expected to differ much from the scatterometer wind in case of high wind gradients. Equally, [9] has shown that the European Centre for Medium-range Weather Forecasts (ECMWF) winds show poor verification in rainy areas and are thus a poor proxy for ASCAT wind data quality. Another problem inherent in scatterometer wind processing near steep gradients resides in the ambiguity removal [12] [13], which is most challenging in variable wind conditions.

In this paper, the SA is further adapted and tested for QC purposes. A complementary approach using both singularity exponent (SE) and MLE is proposed to improve the current ASCAT QC. Section II introduces the different types of wind and rain data sources used in this study. Section III identifies and describes the quality-sensitive parameters, including MLE, the measurement variability factor K_p, and the SE (SA output), independently. A measure of ASCAT wind quality is presented as a function of each mentioned parameter. Here, the mean vector difference (MVD) between ASCAT and ECMWF winds is used as a quality indicator. In Section IV, a complementary QC approach using SE and MLE is first proposed to improve the current ASCAT wind QC. This approach can be further improved by analyzing its performance in separate wind speed and K_p categories, leading to the development of a multidimensional histogram (MUDH) technique. Section V evaluates the performances of the proposed QC approaches (as introduced in Section IV) using collocated ASCAT data and buoy winds, taking account of the enhanced local spatial and temporal wind variability of the QC cases. Finally, the conclusions can be found in Section VI.

II. Data

To study the quality of ASCAT derived winds and the performance of the improved QC, two different collocation data sets are examined, in which ECMWF and buoy winds are used as reference, respectively. ECMWF does not well resolve the wind field in the presence of rain [9]. Buoy data are generally more reliable than ECMWF under rainy conditions, although in case of increased wind variability the buoy wind is less representative of an area mean wind such as that of ASCAT. Therefore, in order to better verify the QC approaches, both data sets should have collocated rain data, either satellite-derived rain rate (RR) or *in situ* measured RR.

The first data set consists of 15 months (September 2008–December 2009) of ASCAT 12.5-km level 2 (L2) data collocated with the Tropical Rainfall Measuring Mission's (TRMM) Microwave Imager (TMI) rain data. The ASCAT data in Binary Universal Format Representation (BUFR) are provided by the European Organisation for the Exploitation of Meteorological Satellites (EUMETSAT) Ocean and Sea Ice (OSI) Satellite Application Facility (SAF). They already include ECMWF winds, which are acquired by time and space interpolation of three 3-hourly ECMWF forecast wind fields on a regular 0.5625° latitude/longitude grid to the ASCAT data acquisition location and time, respectively. The collocation criteria for TMI rain data are less than 30 minutes distance in time and 0.25° distance in space from the ASCAT measurements. Generally, multiple WVCs are collocated with one rain measurement of TMI. The total amount of collocations is about 27 million, with 24.6 million under rain-free conditions and 2.4 million under rainy conditions.

The second data set consists of three years (March 2009–February 2012) of ASCAT 12.5-km L2 BUFR data collocated with tropical moored buoy wind/precipitation data, over the open ocean, and TMI RR data. Since not all the buoys are equipped with a rain gauge, only part of the ASCAT–buoy collocations has rain information. The total amount of collocations in this data set is about 60 thousand, in which only 3600 contain rain information, either buoy RR parameter or TMI RR data. Note that different rain parameters are only used to identify whether a WVC is rain impacted or not, but not for quantitative analysis. The studied buoys include the National Oceanic Atmospheric Administration (NOAA) Tropical Ocean Atmosphere (TAO) buoy arrays in the tropical Pacific, the Japan Agency for Marine-Earth Science and Technology (JAMSTEC) Triangle Trans-Ocean Buoy Network (TRITON) buoys in the western Pacific, the Prediction and Research Moored Array in the Atlantic (PIRATA), and the Research Moored Array for African–Asian–Australian Monsoon Analysis and Prediction (RAMA) at the tropical Indian Ocean. Note that the averaged 2-hourly buoy RR parameter is used in the following section, which is computed from buoy rain gauge time series.

III. Quality-Sensitive Parameters

This section describes three ASCAT quality-sensitive parameters, separately. The goal is to see general trends in data quality. Buoy data are too scarce to show parameter sensitivity to rain and data quality. Thus, the MVD value between ASCAT and ECMWF winds is presented as a function of each parameter for different wind speed and rain conditions, in order to better understand the sensitivity of each parameter to the wind quality. Note that, although the ASCAT wind retrieval quality is known to be somewhat degraded under large small-scale wind variability and heavy rain conditions, Portabella *et al.* [9] show that the ECMWF winds do not resolve at all such conditions. As such, discrepancies between ASCAT and ECMWF can be mainly attributed to the ECMWF model not representing the local convective features. Wind speeds below 4 m/s are not considered in this study, since low winds generally correspond to high vector wind variability and poor wind direction skill, which makes the analysis much more challenging, i.e., beyond the scope of this paper.

A. MLE

For ASCAT, the wind inversion is implemented by searching for the minimum distance between the backscatter triplet and the GMF in a transformed 3-D measurement space (namely z-space), i.e., the following MLE function is minimized [14]:

$$\text{MLE} = \frac{1}{3}\sum_{i=1}^{3}(z_{mi} - z_{si})^2 \tag{1}$$

where $z_{mi} = (\sigma^0_{mi})^{0.625}$ is the backscatter measurement of the ith beam in z-space, and $z_{si} = (\sigma^0_{si})^{0.625}$ is the backscatter simulated through the GMF, i.e., CMOD5n [15], using the solution wind vector as input. In general, the ASCAT backscatter triplets are close to the GMF, corresponding to low inversion residuals or MLE values. To account for noise, the expectation value of the MLE is normalized to one [16]. Occasionally, a large inconsistency with the GMF is induced by geophysical conditions that are not modeled by the GMF, such as increased local wind variability, confused sea state, rain, or land/ice contamination, resulting in large MLE values. Consequently, the MLE is a good indicator of the retrieved wind quality in a WVC. An MLE sign is defined in [8] to improve the MLE-based QC. The sign works as follows: for a given across-track WVC position, by varying wind speed and direction, sets of triple (fore, mid, aft) backscatter measurements simulated through the GMF construct a conical surface in the 3-D measurement space, and hence, each point on the surface depends just on wind speed and direction [14]; triplets located inside the cone surface, i.e., more isotropic than nominal (as depicted by the GMF), are assigned with a positive MLE value, while those located outside the cone are assigned with a negative MLE value. The MLE is generally a proxy for WVC wind variability, where negative and positive MLEs denote stable and unstable flows, respectively. Excessive positive MLEs are generally found near (gust) fronts, squall lines, and convective systems.

Fig. 1 shows the MVD value between ASCAT and ECMWF winds as a function of MLE for different wind speed regions at rain-free and rainy conditions, respectively. There is a clear distinct behavior for MLE values, in terms of wind quality, in both panels. Under rain-free conditions, ASCAT winds retrieved from the triplets inside the cone [associated with positive MLE values in Fig. 1(a)] increase rapidly in MVD as the triplet's distance to the GMF increases. However, for the triplets outside the cone (associated with negative MLE values), the wind vector difference is generally small regardless of the triplet's distance to the cone. In line with this, the current MLE-based QC, which uses a threshold of $+18.6$, to filter poor-quality WVCs works well for the measurements under rain-free condition [8]. Under rainy conditions, ASCAT winds above 4 m/s have rapidly increasing MVD (w.r.t. ECMWF) as the triplet's distance to the cone increases, regardless of the triplet's location. The apparent quality degradation toward negative MLE values is particularly sharp for the wind speed region of [4–7) m/s. This may be understood from the fact that the triplets are moved away from the cone surface due to stable flow (negative MLE), which will, in rainy areas, be associated with relatively dry air descending from the rain clouds and spreading

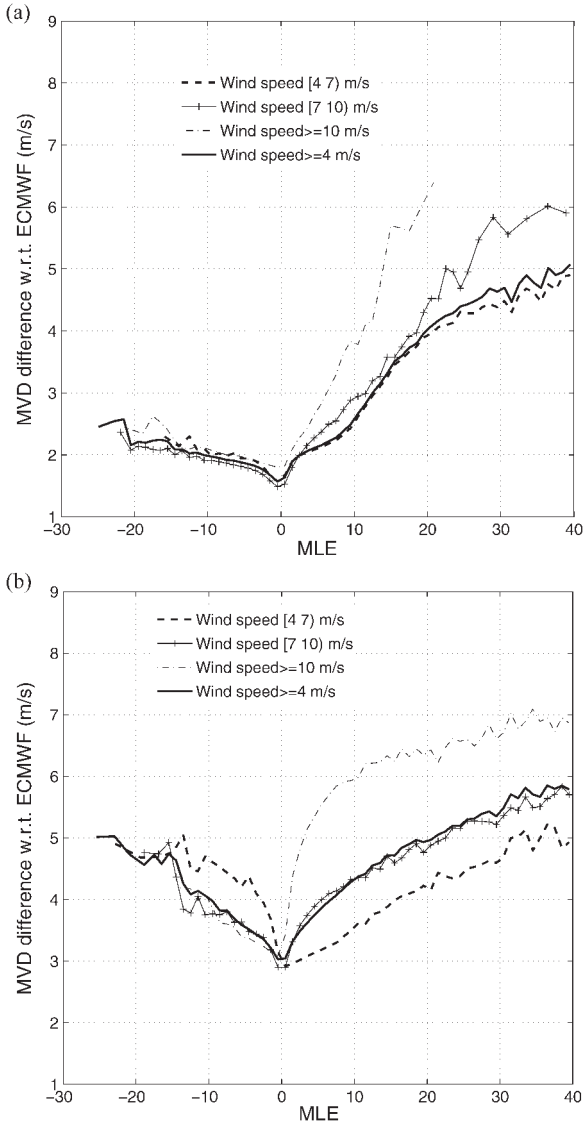

Fig. 1. MVD between ASCAT and ECMWF winds as a function of MLE for (a) TMI rain-free collocated WVCs and (b) TMI rain-contaminated WVCs. The MLE binning is set to be 1. In case that the number of collocations in a studied bin is less than 100, the bin is merged with its closest bin.

over the ocean (convective downbursts), which process is not resolved by the ECMWF model, thus leading to large vector differences.

The vector differences of the current MLE-based QC are summarized in Table I. As discussed in [8], on the one hand, large positive MLE values correspond to increased sub-WVC variability and, in turn, somewhat degraded ASCAT-retrieved wind quality; on the other hand (and as already discussed), increased small-scale wind variability is not resolved at all by ECMWF. MVD scores are consequently high. Therefore, the table mainly indicates the degraded quality in ECMWF winds, in case of ASCAT QC. The total scores of the operational QC are presented in the last row of Table I. Regarding that $\sim 10\%$ of the collocations are with RR > 0 mm/h, it is evaluated that more than two thirds of QC-ed WVCs are in convective areas with rain. In particular, more than 90% of QC-ed WVCs are in variable wind conditions near rain, for the cases with wind

TABLE I
PERCENTAGE AND MVD (M/S) BETWEEN ASCAT AND ECMWF WINDS FOR QC-ACCEPTED AND QC-REJECTED DATA FOR DIFFERENT WIND SPEED REGIONS AND RAIN CONDITIONS USING MLE-BASED (MLE-ONLY) QC

Wind speed(m/s)	TMI rain free			TMI rain contaminated			TMI all weather conditions		
	MVD-Kept	MVD-Rejected	QC-ed ratio(%)	MVD-Kept	MVD-Rejected	QC-ed ratio(%)	MVD-Kept	MVD-Rejected	QC-ed ratio(%)
[4 7)	1.72	4.42	0.18	3.07	4.68	2.18	1.81	4.54	0.31
[7 10)	1.55	5.65	0.04	3.19	5.59	3.10	1.68	5.60	0.29
≥10	1.84	8.40	0.02	3.64	6.90	2.16	2.12	6.95	0.36
≥4	1.67	4.69	0.10	3.28	5.65	2.51	1.80	5.37	0.31

speeds $\geq$ 7 m/s, indicating that convection is the main factor in complicating ASCAT wind verification under these high wind conditions in the tropics.

B. SE

The SE $h(\mathbf{x})$ depicts the degree of local regularity (spatial gradient) around a given point $\mathbf{x}$ for a given scalar signal s. It can be evaluated according to the following function [17], [18]:

$$\frac{1}{r}\left|s(\mathbf{x}+r)-s(\mathbf{x})\right| = \alpha(\mathbf{x})r^{h(\mathbf{x})} + o\left(r^{h(\mathbf{x})}\right) \qquad (2)$$

where $\alpha(\mathbf{x})$ is a dimensional and signal-dependent amplitude factor, and the factor $o(r^{h(\mathbf{x})})$ means a quantity that decreases to zero faster than $r^{h(\mathbf{x})}$ when r goes to 0. The left part of (1) is the gradient estimated at the radius r. Therefore, the SE roughly behaves as

$$h(\mathbf{x}) \sim \frac{\log|\nabla s|(\mathbf{x})}{\log r}. \qquad (3)$$

The numerical implementation of the aforementioned function is described in [19]. Negative SE values correspond to less regular behavior of the function, while positive SE values indicate a more regular behavior. The SA algorithm has been adapted and optimized for the application on ASCAT data in [11]. At each WVC, the minimum SE value from the wind speed, wind direction, and MLE SEs is used to generate the singularity map.

Since the MLE is generally a proxy for sub-WVC wind variability where large positive MLEs are generally found near (gust) fronts, squall lines, and convective systems, one might expect that the MLE and SE values are inversely proportional and thus redundant. However, note that the MLE is a local measure, whereas SE is based on spatial derivatives between WVCs and therefore may indeed be complementary to MLE values.

Fig. 2 shows the MVD value between ASCAT and ECMWF winds as a function of the SE value derived from [11]. ECMWF winds are less representative of ASCAT winds as the SE value decreases, which is in line with the general smoothness of the ECMWF model near convection [9]. The apparent quality degradation rate is larger at high wind speeds than that at low wind speeds, as the former implies deeper convection. Another interesting result is that WVCs flagged by MLE-based filter and WVCs flagged by SE-based filter with a threshold of -0.45 do generally not coincide (45% of the operationally QC-ed WVCs are with SE < -0.45; while 32% of the WVCs, which correspond to SE < -0.45, are with MLE $> +18.6$), indicating that SE is potentially very complementary to the operational MLE-based QC. In Section IV, SE is further used to complement the current MLE-based QC. Then, a more comprehensive study using SE, MLE, K_p, and wind speed is developed to refine the complementary QC approach.

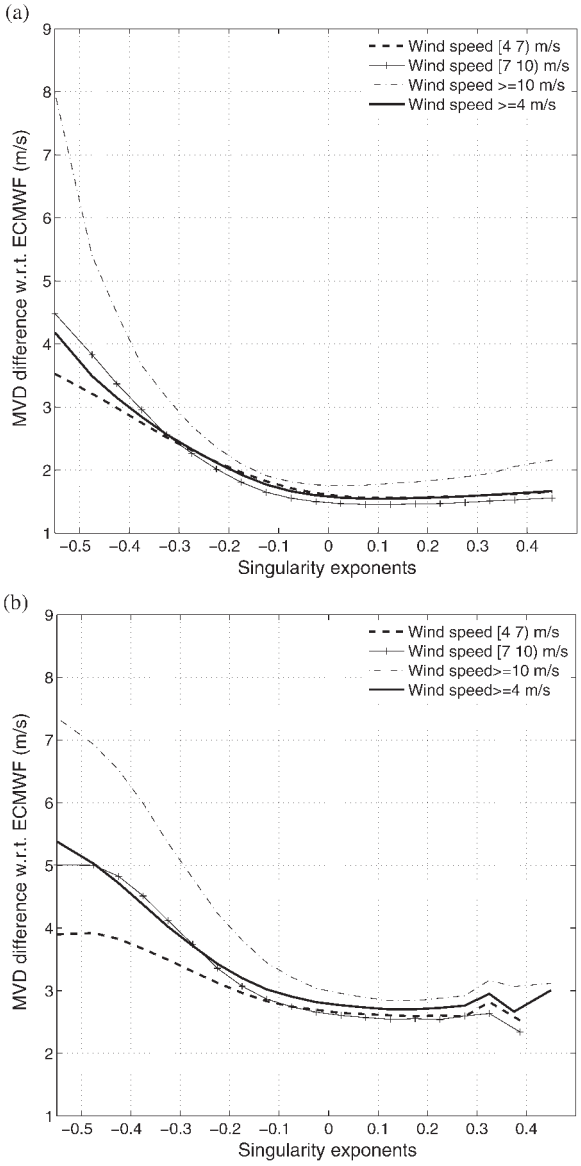

Fig. 2. Vector difference between ASCAT and ECMWF winds as a function of SE (bins of 0.05) for (a) TMI rain-free collocated WVCs and (b) TMI rain-contaminated WVCs.

C. Measurement Variability Factor (K_p)

The variability of ASCAT backscatter σ^0, namely K_p, is defined as the normalized standard deviation (SD) of the measurements, i.e.,

$$K_p = \frac{\sqrt{\mathrm{var}(\sigma^0)}}{\overline{\sigma^0}} \tag{4}$$

where $\overline{\sigma^0}$ is the mean backscatter of a beam in a WVC, and $\mathrm{var}(\sigma^0)$ is its estimated variance. The K_p value can be regarded as a measure of the error in the mean backscatter caused by speckle noise, instrument characteristics, data processing, and spatial heterogeneities of the target [20], such as wind variability.

Similar to Fig. 1, the behavior of K_p, in terms of wind MVD, is shown in Fig. 3 for rain-free and rainy conditions separately, in which the horizontal axis indicates the mean K_p value of the fore and aft beams. As expected, the MVD value generally increases as the measurement error increases. The apparent wind quality degradation rate in Fig. 3 is smaller than that in Fig. 1, except for wind speeds ≥ 10 m/s under rain conditions. This indicates that K_p may be helpful to detect spatially variable weather conditions. In Section IV-B, K_p is adopted by the MUDH QC algorithm to improve the rejecting of poor-quality winds.

IV. Improved QC

Although the vector difference between ASCAT and ECMWF is not necessarily a good indication of ASCAT quality, it does indicate extreme wind variability and convection, where SE (as MLE) may be effective in detecting unrepresentative ASCAT winds, and it is therefore used below. This section presents two approaches to improve the single parameter (MLE)-based QC. The first one is based on a combination of the SE and the MLE. The second methodology uses all the mentioned quality-sensitive parameters in Section III (including SE, MLE, K_p, and wind speed) to develop a MUDH QC flag. The idea behind these two approaches is as follows: the MVD value between ASCAT and ECMWF winds is estimated in a 2-D (first approach) or 4-D (second approach) space. Then, a flag table is derived, by setting the 2-D or 4-D bins whose MVD is higher than the threshold T_{MVD} to be flagged and setting the bins whose MVD is lower than T_{MVD} to be unflagged. Note that we do not intend to perform QC for WVCs with MLE values less than $+18.6$ and SE values larger than -0.2. Due to the lack of data in certain bins, the corresponding MVD values may be extremely high or low, leading to isolated flag bins in the table. A neighbor filtering is then applied to the flag table. If the number of data in a certain bin is higher than 50, its corresponding flag value is kept. Otherwise, if the MVD value of this bin is above the threshold value T_{MVD}, the bin is initially set as QC flagged. Then, the number of adjacent bins within a 3×3 box, which are set to filter data, is accounted for. If more than half of the adjacent bins are set as QC flagged, we consider it to be sufficient evidence for rejecting winds associated with this bin, or else we leave the flag unset for this bin. Finally, the processor simply uses the derived quality-sensitive parameters, converts them into table indexes, and checks for the corresponding bin value in the flag table. The flag tables are further validated using collocated ASCAT and buoy data in Section V.

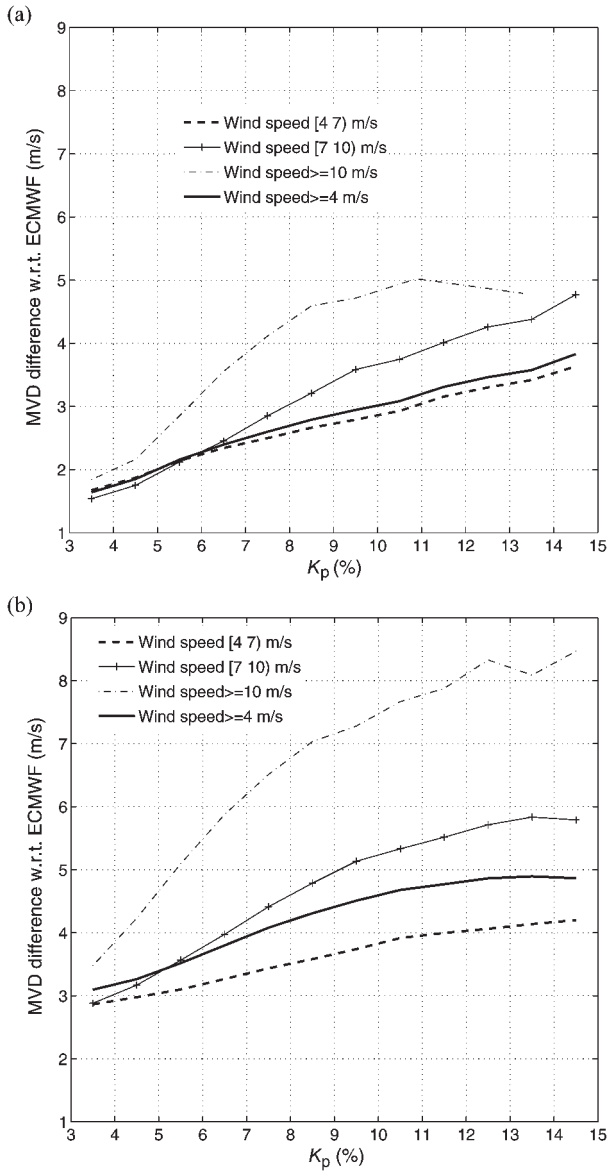

Fig. 3. Vector difference between ASCAT and ECMWF winds as a function of K_p (bins of 1%) for (a) TMI rain-free collocated WVCs and (b) TMI rain-contaminated WVCs.

A. Combined SE/MLE Analysis

As introduced in [11] and mentioned earlier, SE is complementary to MLE in terms of QC. Fig. 4(a) shows the MVD value as a function of SE and MLE for wind speeds above 4 m/s. The white areas are due to the lack of data in the corresponding bins, in which the number of collocations is less than five. It is consistent with the established fact that ASCAT wind quality generally decreases as the MLE value increases, and it shows increased MVD as the SE value decreases. Large MVD values occur for a set of ASCAT winds derived from triplets that are

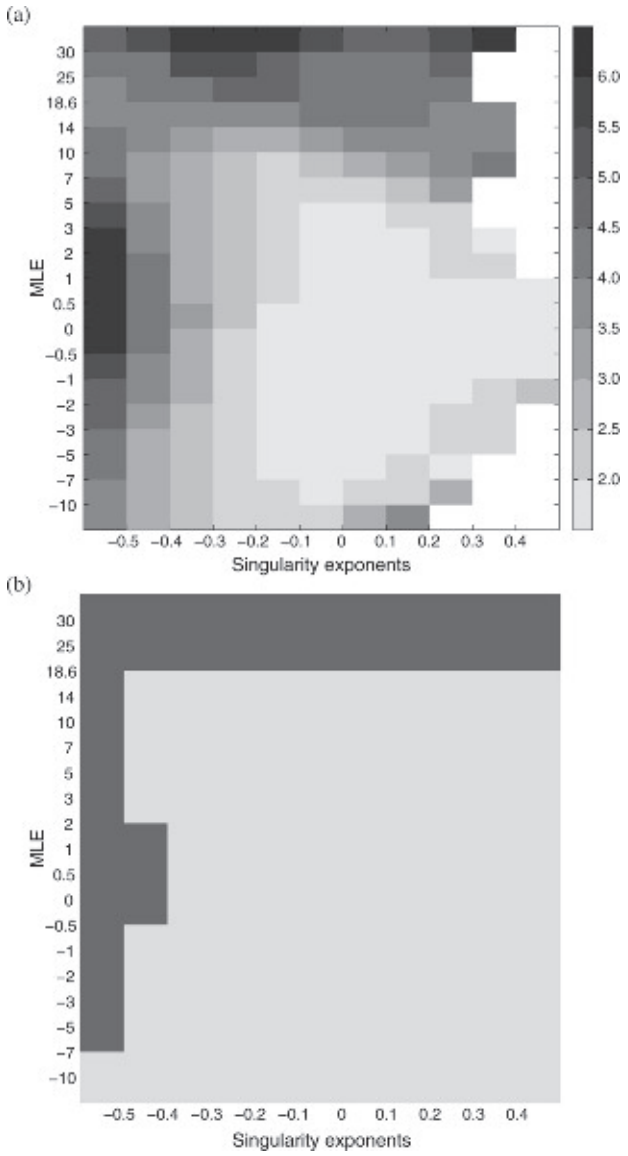

Fig. 4. (a) Vector difference between ASCAT and ECMWF winds as a function of SE and MLE. The blank area is due to the lack of data in the corresponding bins. The grayscale corresponds to different MVD values (see the legend). (b) Simple QC flag table derived from Fig. 4(a). The dark gray corresponds to the bins set for filtering (QC-rejection criterion); the light gray corresponds to the bins unset for filtering (QC-acceptance criterion).

close to the GMF cone surface (low absolute MLE value and low SE value) that are now detected by the combined analysis, but which have not been examined before.

A threshold of $T_{\mathrm{MVD}} = 4.5$ m/s is used to produce the flag table [see Fig. 4(b)]. To inherit the current QC, WVCs with MLE above $+18.6$ are always rejected. The dark gray corresponds to the bins set for filtering (QC-rejection criterion), while the light gray corresponds to the bins unset for filtering (QC-acceptance criterion). A verification of this QC approach is summarized in Table II. When compared with the MLE-based QC statistics in Table I, it is clear that, in general, the new algorithm is rejecting more points than the MLE-based QC. By construction, the MVD scores for rejected data are comparable in both algorithms, since MVD values will be large for low SE mainly due to the large spatial representativeness error of the ECMWF winds near convection. Therefore, the new algorithm rejects many more winds near rain at low and moderate wind speed ($v < 10$ m/s) categories. For wind speeds below 10 m/s, the MVD scores of rejected WVCs are slightly lower than those rejected by the MLE-based QC, while for wind speeds above 10 m/s, the MVD scores are higher.

The rain impact on MVD wind difference can also be understood using the combined SE/MLE analysis. Fig. 5 shows the mean TMI RR as a function of SE and MLE value. Similar to the vector difference between ASCAT and ECMWF winds, the mean TMI RR increases as the triplet's distance to the cone surface increases and the SE value decreases, indicating that more rain is present for both high sub-WVC variability (MLE) and high inter-WVC variability (low SE). Hence, high rain rates associate well with small SE values and large MLE values.

One should also note that the distribution of large mean TMI RR does not align exactly with the MVD score in Fig. 4. The MVD values in Fig. 4 are most likely due to the local increase of wind variability, which is mostly associated with rain events. However, as already mentioned, ECMWF does not well resolve the ocean wind field under rainy conditions. As such, other independent and reliable wind sources, such as buoy winds, should be used to assess the ASCAT wind quality in the presence of rain (see Section V).

B. MUDH Technique

To refine the QC approach introduced in Section IV-A, an extended analysis is presented here by also taking the measurement variability (K_p) and wind speed parameters into account, leading to the development of the MUDH technique. MUDH was first developed in the context of scatterometry to flag rain contamination for SeaWinds on QuikSCAT [2]. It identifies parameters that are sensitive to rain, estimates the probability of rain as a function of them using a training data set, and then uses the rain probability to flag for rain. MUDH is adapted here to improve ASCAT QC. As such, the MVD value between ASCAT and ECMWF winds, instead of the rain probability, is estimated during the development of MUDH for ASCAT. Then, a MVD threshold introduced before is used to flag data.

Fig. 6 illustrates the ASCAT MVD scores as a function of SE and MLE for the categories of moderate wind speed/small K_p value, moderate wind speed/large K_p value, high wind speed/small K_p value, and high wind speed/large K_p value, respectively. The white areas are due to the lack of data in the corresponding bins (number of data < 5). The behavior of SE and MLE, in terms of wind vector difference, clearly varies with K_p and wind speed. On the one hand, the causes for increased MVD scores are different for each category. For instance, convection is the main cause of apparent quality degradation for the category of high wind speed and large K_p value, in which the mean rain rate is generally higher than 3 mm/h (not shown) over all the SE/MLE bins, and thus, more convective activity is present. Since the winds are high, the large MVD value is likely due to large ECMWF errors and sub-WVC wind variability effects on ASCAT-retrieved quality. The large MVD distributions in Fig. 6(b) and (c) are also associated with relatively high mean TMI RR (not shown). However, the mean

TABLE II
PERCENTAGE AND MEAN MVD VALUE BETWEEN ASCAT AND ECMWF WINDS FOR QC-ACCEPTED AND QC-REJECTED WVCS USING THE COMBINED SE/MLE FLAG TABLE IN FIG. 4

Wind speed(m/s)	TMI rain free			TMI rain contaminated			TMI all weather conditions		
	MVD-Kept	MVD-Rejected	QC-ed ratio(%)	MVD-Kept	MVD-Rejected	QC-ed ratio(%)	MVD-Kept	MVD-Rejected	QC-ed ratio(%)
[4 7)	1.71	4.03	0.33	3.03	4.47	5.02	1.80	4.26	0.64
[7 10)	1.54	4.83	0.09	3.12	5.53	5.74	1.67	5.43	0.55
≥10	1.83	7.13	0.06	3.56	7.35	3.94	2.10	7.34	0.69
≥4	1.66	4.32	0.19	3.22	5.58	4.97	1.79	5.22	0.61

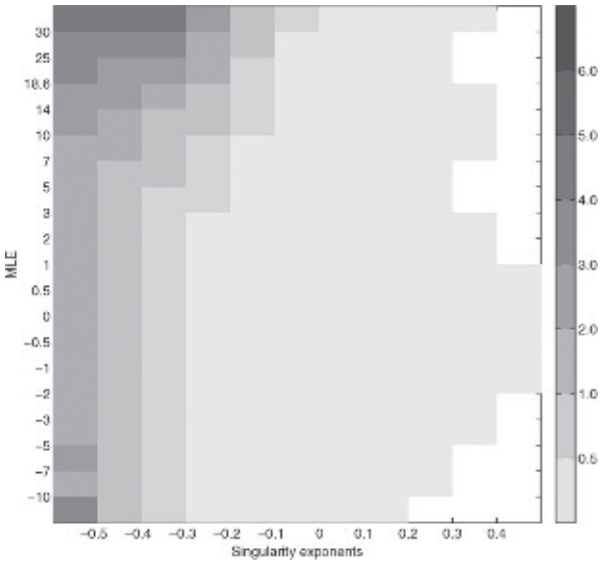

Fig. 5. Mean TMI RR as a function of SE and MLE. Only the collocations with wind speeds above 4 m/s are used.

TMI RR is really low for the category of low wind speed and small K_p value [less than 0.5 mm/h for all the SE/MLE bins, except for those bins in the left lower corner of Fig. 6(a)]. In addition, here, the elevated MVD scores may be caused by increased local wind variability. On the other hand, the rain splash produces different effects on MLE for different wind speed conditions. Apparent poor-quality winds induced by rain are generally associated with low negative MLE values under low wind speeds [see the lower left corner of Fig. 6(b)] and associated with only small effects at high wind speeds.

To implement the MUDH QC approach, the binning of MLE and SE is set according to the axis labels of Fig. 6. The wind speeds are roughly separated into three categories, i.e., $4 \leq v < 7$ m/s; $7 \leq v < 10$ m/s; and $v \geq 10$ m/s. The K_p (mean value of the fore—and aft-beams) bins are set as follows: $K_p < 3\%$, $K_p \geq 15\%$, and bins of 2% for K_p in the range [3% 15%). Since the MVD scores depend on wind speed, a set of thresholds $T_{\mathrm{MVD}} = 4.0$, 4.4, and 6.2 m/s are used for the wind speed categories $4 \leq v < 7$ m/s, $7 \leq v < 10$ m/s, and $v \geq 10$ m/s, respectively, in order to produce the multidimensional QC flag table and account for the variable ECMWF errors. A verification of the MUDH technique on ASCAT QC is summarized in Table III, which can be compared to that of the MLE-based QC (see Table I) and the SE/MLE QC (see Table II). It shows that the MUDH technique rejects nearly three times as many WVCs as the MLE-based QC and 50% more than the SE/MLE QC, while the MVD value of the rejected WVCs is similar for the three QC techniques. Similar conclusions can be drawn when splitting the analysis into different wind speed categories. Moreover, MUDH rejects many more ASCAT measurements in variable wind areas with rain, particularly for wind speeds below 7 m/s.

V. VALIDATION RESULTS

A. Validation With 10-min Buoy Wind Measurements

As discussed in Section IV, in [9], Portabella *et al.* show that ECMWF does not well resolve the rain-induced wind flow and, as such, is not a reliable wind reference for assessing the ASCAT QC in the presence of convection. To better assess the performance of the proposed complementary QC algorithms, an independent wind source, such as buoy data, is required. However, since the number of ASCAT–buoy collocations (particularly those with rain information) is much smaller than that of ASCAT–TMI collocations, it is not possible to make an as thorough analysis as in Section IV. Consequently, a set of larger MLE bins is used here.

Fig. 7(a) shows the MVD value between ASCAT and buoy (solid), ASCAT and ECMWF (dashed), for the collocations of the second data set (ASCAT–ECMWF–Buoy), as introduced in Section II. It confirms that WVCs with the most negative SEs are in areas with large wind variability, as expected. The dash-dotted line associated to the right y-axis shows the percentage of rainy collocations with RR ≥ 3 mm/h. As before, high probability of rain is found for the most negative SEs indicating high WVC variability. In general, the reduced correspondence of buoy, ASCAT, and ECMWF winds with decreasing SE values is further confirmed. Fig. 7(b) presents the MVD value between ASCAT and buoy winds as a function of SE and MLE. It shows a similar pattern to that in Fig. 4(a), which again indicates that SE and MLE parameters are complementary in terms of QC.

Table IV presents the QC results of the collocated ASCAT–buoy data set using the three mentioned methods, i.e., the current MLE-based QC (threshold of $+18.6$), the combined SE/MLE analysis, and the MUDH technique. Regarding the complementary QC approaches, the flag tables derived in Section IV (using collocated ASCAT–ECMWF–TMI data set) are used to filter the data set with collocated ASCAT–buoy measurements. Buoy winds are adopted as reference in the statistics.

The percentage of QC-rejected WVCs in the second data set is similar to those presented in Tables I–III. The simple

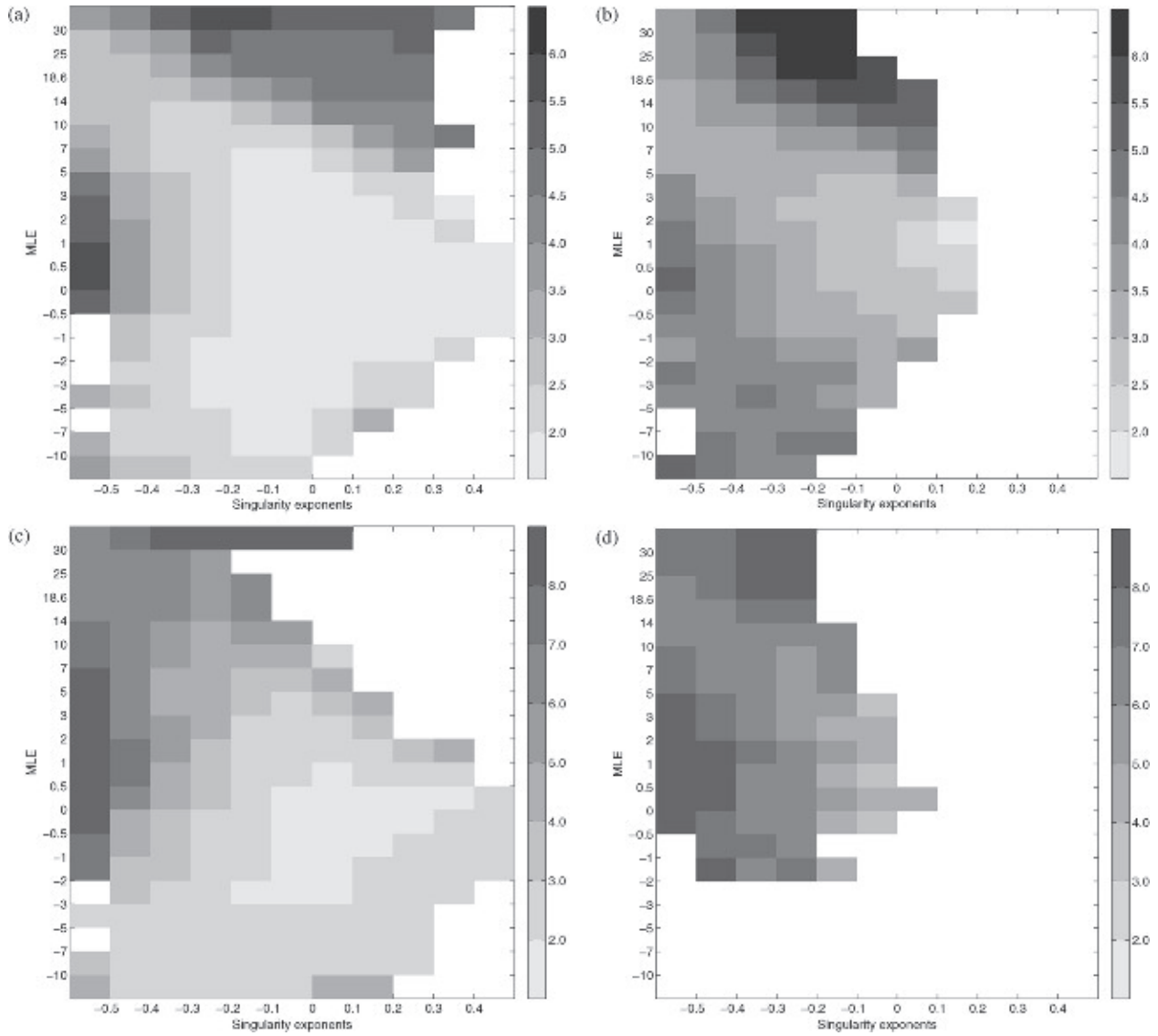

Fig. 6. Vector difference between ASCAT and ECMWF winds as a function of SE and MLE for (a) moderate wind speeds ($4 \leq v < 7$ m/s) and small K_p values ($K_p < 4\%$); (b) moderate wind speeds ($4 \leq v < 7$ m/s) and large K_p values ($K_p > 7\%$); (c) high wind speeds ($v > 10$ m/s) and small K_p values ($K_p < 4\%$); and (d) high wind speeds ($v > 10$ m/s) and large K_p values ($K_p > 7\%$). The gray scale indicates the MVD values (see the legend); the blank area is due to the lack of data in the corresponding bins.

TABLE III
PERCENTAGE AND MVD VALUE BETWEEN ASCAT AND ECMWF WINDS FOR QC-ACCEPTED AND QC-REJECTED DATA USING THE MUDH ALGORITHM

Wind speed(m/s)	TMI rain free			TMI rain contaminated			TMI all weather conditions		
	MVD-Kept	MVD-Rejected	QC-ed ratio(%)	MVD-Kept	MVD-Rejected	QC-ed ratio(%)	MVD-Kept	MVD-Rejected	QC-ed ratio(%)
[4 7)	1.71	3.96	0.44	2.98	4.49	8.32	1.79	4.26	0.96
[7 10)	1.54	4.61	0.13	3.04	5.63	8.38	1.66	5.48	0.80
≥10	1.83	7.00	0.08	3.52	7.35	5.02	2.10	7.32	0.88
≥4	1.66	4.22	0.26	3.16	5.53	7.39	1.78	5.17	0.88

combination of SE and MLE rejects twice as many WVCs as the MLE-based method, while the MUDH algorithm rejects three times more data. In contrast with the MVD scores of the QC-ed WVCs in Tables I–III, the rejected WVCs with the new approaches have a higher MVD score (see the upper row in each wind speed category) than those rejected by the MLE-based method, indicating that the algorithms proposed in Section IV are very effective in rejecting spatially variable winds over all of the wind speed regions.

The verification of the MUDH algorithm on the 3000 ASCAT–buoy–ECMWF collocations with rain information is presented in Table V. The conclusion is the same as per

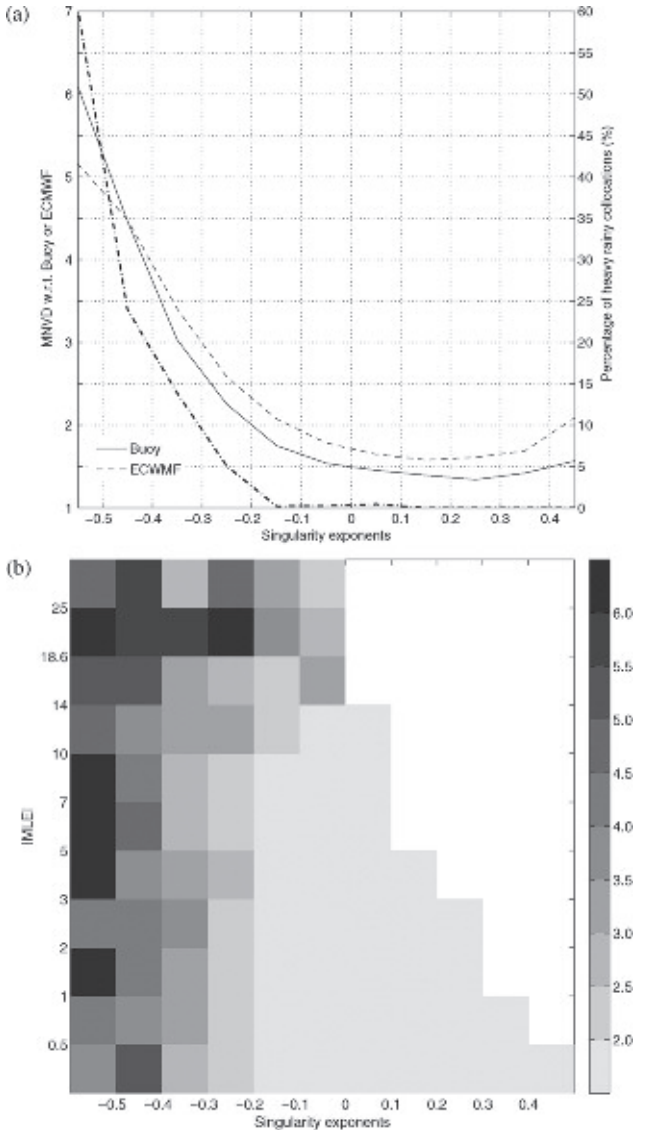

Fig. 7. (a) Vector difference between ASCAT and buoy winds (thin solid); ASCAT and ECMWF winds (dashed); the dash-dotted line shows the percentage of rain-contaminated WVCs (TMI RR or averaged 2-hourly buoy RR $\geq$ 3 mm/h) in each bin for the 3000 ASCAT–buoy collocations with rain information. (b) MVD value between ASCAT and buoy winds as a function of SE and MLE.

Table III, i.e., the rejected rain-free ASCAT winds compare worse to buoys than the nonrejected rain-contaminated winds. It proves that the MUDH algorithm is effective in detecting WVCs with enhanced variability in both rainy and rain-free conditions.

B. Validation With 25-km-Equivalent Buoy Winds

The 10-min buoy wind point measurement is not representative of the scatterometer 25-km area-mean measurement in case of large sub-WVC wind variability, which usually corresponds to quality-controlled ASCAT retrieved winds. However, buoy wind time series can be used to estimate 25-km equivalent WVC winds. That is, 10-min continuous buoy wind series are averaged to 25-km-equivalent scale and used as reference in the validation. The mean wind direction is computed as follows:

$$\overline{\varphi} = \arctan\left(\frac{-\overline{u}}{-\overline{v}}\right) \tag{5}$$

where the mean wind components are calculated using the following equations:

$$\begin{cases} \overline{u} = \frac{1}{M}\sum_{i=1}^{M} -w_i \sin(\varphi_i) \\ \overline{v} = \frac{1}{M}\sum_{i=1}^{M} -w_i \cos(\varphi_i) \end{cases} \tag{6}$$

where M is the number of 10-min buoy measurements, which is determined by expanding the 10-min-equivalent distance vector in the adjacent time bins (centered on the ASCAT measurement time), until the length of the distance vector reaches the WVC size. The minimum value M is set to be 5 (i.e., buoy time series averages within ± 20 min of the ASCAT measurement time). w_i and φ_i represent the wind speed and direction of the ith measurement, respectively. The mean wind speed can be derived using either

$$\bar{w} = \sqrt{\bar{u}^2 + \bar{v}^2} \tag{7}$$

$$\bar{w} = \frac{1}{M}\sum_{i=1}^{M} w_i. \tag{8}$$

In the presence of large sub-WVC wind variability conditions, the mean wind speed estimated by (7) is usually lower than that estimated by (8). The latter is more representative of the scatterometer measurements since it well correlates with the integrated sea-surface roughness within the WVC. For example, highly variable winds, i.e., blowing at very different and opposed wind directions, lead to very low mean wind speed according to (7) (average of the wind components) and relatively higher mean wind speed according to (8) (average of the wind speeds). The scatterometer receives energy from the different sea-surface wind/roughness contributors within the WVC and, as such, well correlates with (8). In this paper, the mean buoy wind speed is therefore calculated using (8).

In Table VI, the mean SDs of the continuous buoy wind components are presented for the operational QC-ed WVCs, SE/MLE QC-ed WVCs, MUDH QC-ed WVCs, and for WVCs with $|\text{MLE}| < 0.5$ and $\text{SE} > 0$. It shows that the proposed QC methods are rejecting WVCs with similar high sub-WVC wind variability than those rejected by the MLE-based QC. High inter-WVC variability generally implies high sub-WVC variability and vice versa, such that SE and MLE both detect (extremely) high wind variability cases. However, the SE and MLE thresholds imply different tradeoffs between detection probability and false alarm rate, i.e., a fraction of the high wind variability cases is detected by SE but not by MLE and vice versa. As expected, the rejected WVCs by the different QC approaches have much higher local wind variability than those with $|\text{MLE}| < 0.5$ and $\text{SE} > 0$ (last row), further confirming that combining MLE and SE results in a good wind variability indicator.

Table VII presents the same MVD scores than the last row of Table IV, but using the 25-km-equivalent buoy winds instead of the 10-min buoy winds as reference. The MVD

TABLE IV
VECTOR DIFFERENCE BETWEEN ASCAT AND BUOY WINDS FOR THREE DIFFERENT QC METHODS

Wind speed (m/s)	MVD of rejected WVCs (m/s)			MVD of kept WVCs (m/s)			QC-ed ratio (%)		
	MLE	SE/MLE	MUDH	MLE	SE/MLE	MUDH	MLE	SE/MLE	MUDH
$4 \le v < 7$	4.07	4.12	4.18	1.53	1.52	1.51	0.31	0.66	1.12
$7 \le v < 10$	5.08	5.28	5.28	1.53	1.52	1.51	0.37	0.68	1.08
$v \ge 10$	7.32	7.81	7.68	1.98	1.95	1.94	0.24	0.56	0.81
$v \ge 4$	5.04	5.28	5.21	1.63	1.62	1.61	0.32	0.65	1.04

TABLE V
VECTOR DIFFERENCE BETWEEN ASCAT AND BUOY WINDS FOR QC-ACCEPTED AND QC-REJECTED DATA USING THE MUDH ALGORITHM UNDER DIFFERENT RAIN CONDITIONS

Wind speed (m/s)	Rain free		Rainy	
	MVD-Kept	MVD-Rejected	MVD-Kept	MVD-Rejected
$v \ge 4$	1.48	3.11	2.58	5.58

TABLE VI
MEAN SD VALUES OF THE CONTINUOUS BUOY WIND COMPONENTS FOR DIFFERENT CATEGORIES

	SD (speed, m/s)	SD (direction, °)	SD (u, m/s)	SD (v, m/s)
MLE	1.24	27.7	1.66	1.62
SE/MLE	1.27	32.1	1.62	1.61
MUDH	1.29	34.9	1.60	1.73
$\lvert$MLE$\rvert<0.5$, SE>0	0.37	6.3	0.47	0.52

TABLE VII
VECTOR DIFFERENCE BETWEEN ASCAT AND 25-km-EQUIVALENT BUOY WINDS FOR THREE DIFFERENT QC METHODS

Wind speed (m/s)	MVD of rejected WVCs (m/s)			MVD of kept WVCs (m/s)		
$v \ge 4$	MLE	SE/MLE	MUDH	MLE	SE/MLE	MUDH
	4.14	4.34	4.39	1.29	1.28	1.27

scores are smaller in Table VII than in Table IV (last row), indicating that the 25-km-equivalent buoy winds are indeed more representative of ASCAT winds than the 10-min buoy wind point measurements, notably in high wind variability conditions (i.e., the rejected WVCs). In [21], Vogelzang *et al.* estimated the quality of ASCAT and 10-min buoy winds on the scatterometer scale and found that the buoy error variance contribution to the vector difference variance is 72% while the ASCAT 12.5-km contribution is only 28% for the accepted WVCs, i.e., scatterometer winds are, in general, of much higher quality than buoy point-measurement winds at scatterometer scales. The time averaging presented here reduces the variance of the ASCAT and buoy vector difference around 15.2% and 15.8% for accepted and rejected WVCs, respectively. Following [20], this would imply that the time-averaged buoy error and the ASCAT 12.5-km contribution would be respectively 67% and 33% for accepted WVCs, i.e., scatterometer winds are, in general, of more similar quality to that of time-averaged buoy winds at scatterometer scales. Temporally averaged buoy winds thus do clearly better represent 25-km spatially averaged winds. Since the time averaging reduces both the rejected and accepted WVC variances in similar amounts, also for the rejected cases the wind variances appear rather scalable and wind errors appear mainly due to enhanced wind variability rather than rain contamination and other effects associated with convection. In other words, the MVD scores are dominated by wind representativeness errors, which explains the large vector differences between accepted and rejected WVCs. As such, all wind measurements (ASCAT, buoys, and ECMWF) are expected to be of lower quality for rejected cases than the equivalent qualities for accepted WVCs.

C. Test Case

Fig. 8(a) shows an ASCAT wind field with TMI RR values superimposed. The operational QC rejects some WVCs under heavy rain (see the gray arrows around 6.0° N and 177.5° E), but which appear quite consistent spatially. Many other WVCs with more or less rain are not rejected, but which are more erratic. As presented in [9], a more constrained MLE threshold may not be effective in rejecting the wind artifacts. For example, at the position denoted by a triangle (where TMI RR $= 8.9$ mm/h), the ASCAT wind inversion residual is relatively low (MLE $= -5.5$) and the retrieved wind speed and direction are 5.51 m/s and 15.3°, respectively. While the collocated buoy measurement shows a wind speed $= 3.4$ m/s, and wind direction $= 280°$ (the temporally averaged buoy wind and direction are 4.1 m/s and 265.5°, respectively), indicating that the ASCAT-retrieved wind is not representative of the buoy wind over there. Fig. 8(b) illustrates the time series of 10-min buoy winds (see the solid line with triangle markers) as compared to the ASCAT measurement (see the square marker, first-rank/selected solution; and the circle marker, second-rank solution) for this particular ASCAT–buoy collocation.

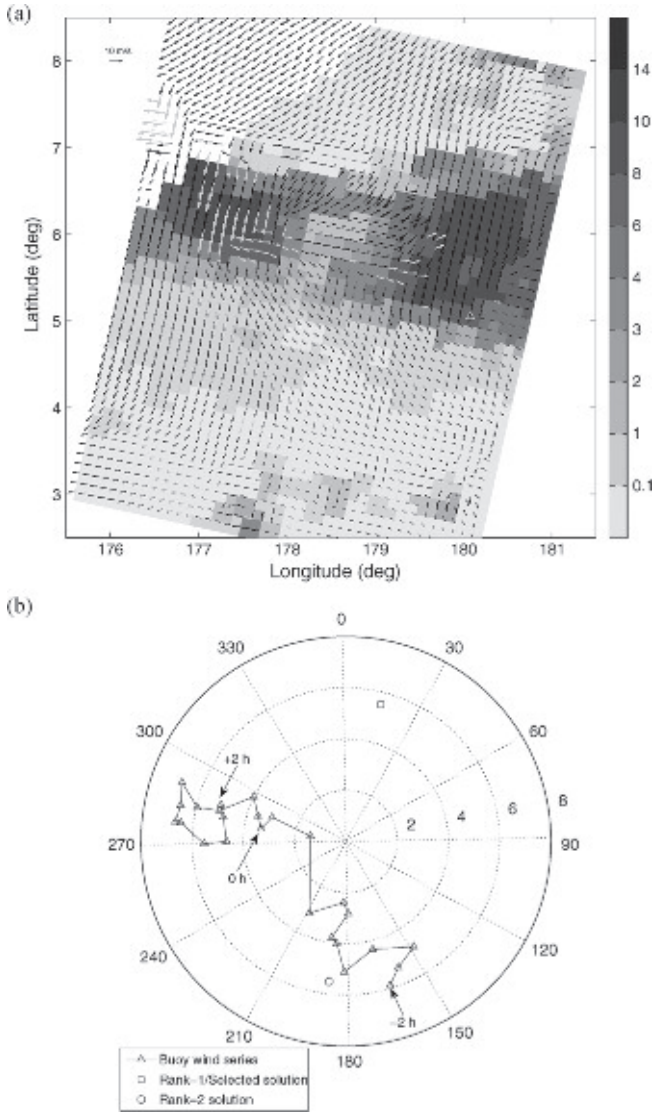

Fig. 8. (a) ASCAT wind observed on December 15, 2009, at 21:17 UTC, with collocated TMI RR superimposed (see the legend). The black arrows correspond to QC-accepted WVCs, and the gray arrows correspond to QC-rejected WVCs. The buoy measurements (denoted by the triangle) were acquired at $21:20 \pm 2$ hours UTC, as shown in the polar coordinate plot (b). The square marker indicates the ASCAT first-rank solution, which is also the selected solution; the circle marker shows the ASCAT second-rank solution.

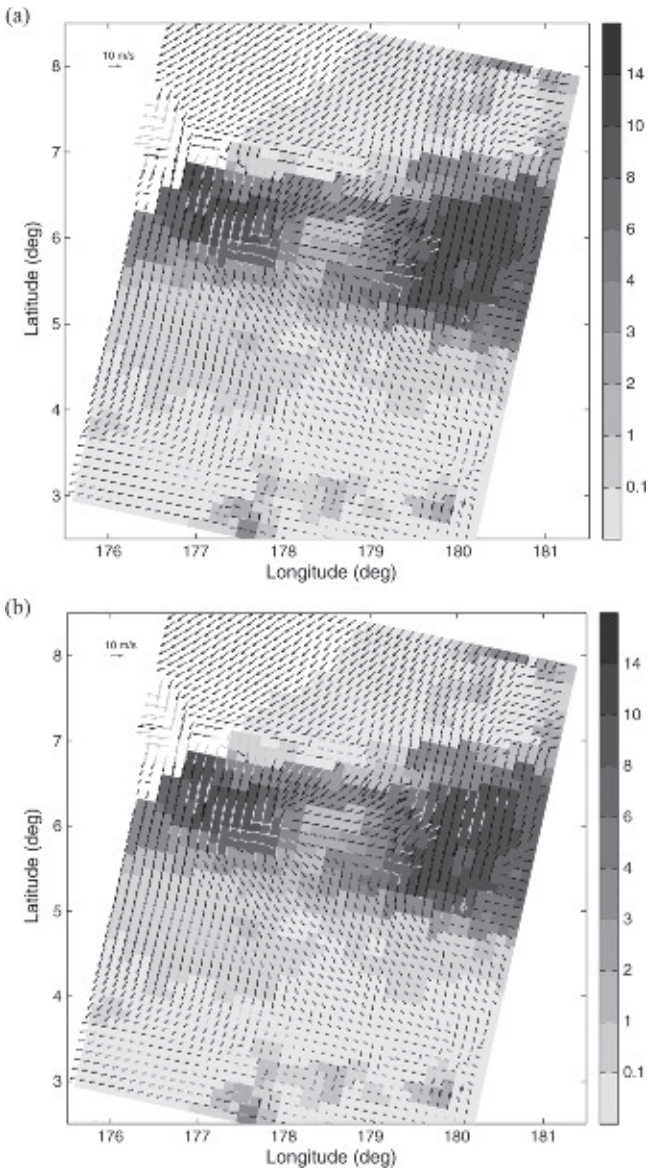

Fig. 9. Illustration of the rejected WVCs (gray arrows) using (a) the combined SE/MLE analysis and (b) the MUDH technique. The gray ones correspond to QC-rejected WVCs. The buoy measurements (denoted by the triangle) were acquired at 21:00 UTC.

Fig. 9(a) and (b) illustrate the rejected winds (gray arrows) using the QC methods that are presented in Section IV-A and B, respectively. It is clear that the new methods reject more WVCs than the operational QC in rainy regions and their vicinity, in line with the increased wind variability denoted by SE. The MUDH algorithm indeed filters more WVCs than the SE/MLE (e.g., the areas around 2.9° N and 177.5° E, 6.2° N, and 180° E). The WVC at the position denoted by a triangle, which corresponds to high wind variability, is also rejected by the MUDH technique.

D. Discussion

Spatial and temporal wind representativeness are dominating the quality indexes, therefore posing a challenge in verification of the QC scheme. Moreover, where rain is spatially erratic, it induces downbursts of wind on the ocean surface with strong gust fronts, and as such, rain is associated with enhanced wind variability. Wind verification of a QC scheme by buoy data thus may be penalizing conditions with such high wind variability, since the wind vector measured at a buoy location is generally expected to differ much from the scatterometer wind in case of high wind gradients.

The already discussed MVD scores after buoy temporal averaging suggest that indeed buoy errors increase with wind variability since a 1-D or 1-D (temporal) averaging becomes less representative of a true 2-D WVC-mean wind (i.e., ideally measurable by spatially averaging a set of buoys evenly distributed over a 25-km WVC) as the subcell wind variability increases, although more representative than a buoy point measurement. However, to conclude on the actual contribution of both ASCAT and buoy wind errors to the high MVD scores

shown in Table VII (rejected category), further analysis is required, e.g., triple collocation [21]. We may already note that the quality of the rejected WVCs is not the same for the three wind data sources. In particular, ECMWF winds are shown in [9] to be of very poor quality under high wind variability conditions.

Since the time averaging of buoy winds reduces both the rejected and accepted variances in similar amounts, wind variances appear scalable and wind errors appear mainly due to enhanced wind variability for the rejected cases, i.e., wind representativeness errors dominate the vector differences between ASCAT and buoy winds. Therefore, all wind measures (ASCAT, buoys, and ECMWF) are expected to be of lower quality than the equivalent qualities in kept WVCs. While it is clear that, at scatterometer scales, ECMWF wind errors are high and buoy errors considerably increase under large subcell wind variability, ASCAT errors remain unassessed.

VI. Conclusion

In this paper, the correlation between the ASCAT wind quality and a few ASCAT-derived parameters, i.e., MLE, K_p, and SE, has been investigated. The three parameters are indeed well correlated with wind quality, which is dominated by wind variability. In order to improve the rejection of poor-quality ASCAT winds, two new algorithms are proposed, which combine the MLE with other quality-sensitive parameters.

The combination of SE and MLE is first investigated. The SE is proven to be a complementary parameter to MLE for ASCAT QC purposes, particularly in finding large sub-WVC variability cases under rainy conditions. This method has been refined by taking the K_p and wind speed parameters into account, leading to the development of the MUDH algorithm. The multiparameter-based QC approaches are developed using ECMWF wind reference and validated using buoy wind reference. The 10-min buoy validation results show that the proposed SE/MLE and MUDH methods filter, respectively, twice and three times as many WVCs than the current MLE-based QC for ASCAT wind speeds above 4 m/s. In particular, more data are rejected by the new methods near convection (rain). The rejected WVCs compare as poor to buoys as those screened by the operational MLE-based method.

A method to convert 10-min buoy wind data to 25-km-equivalent winds is proposed and used for QC verification. Temporally averaged buoy winds do clearly better represent 25-km spatially averaged winds. As already mentioned, the ASCAT wind quality seems to be mainly associated with large (sub-WVC) wind variability. Further work to quantify independent ASCAT, buoy, and ECMWF wind errors (e.g., triple collocation analysis) needs to be carried out. In addition, no evidence of a rain splashing signature and/or other effects associated with convection (e.g., sea state) has been found in this study. Future work will focus on determining whether these effects do significantly contribute to ASCAT wind quality degradation or not, notably at low winds.

Further analysis is required when applying the proposed method on 25-km ASCAT products. Although the edge effects of SA have been reduced by the description in [11], its performance has not yet been examined specifically. Furthermore, future work will also focus on analyzing the correlation between singularity fronts and ASCAT backscatter measurements, in particular which have not yet been adopted by the SA. For such purpose, ASCAT level 1b full-resolution backscatter data will be exploited, since at smaller footprints the rain splashing signal (among other nonwind signals), being patchy and intermittent, is expected to become more evident.

It is found that the proposed methods are effective in detecting variable winds over all the wind speed and RR regimes. Variable winds are a potential hazard in some applications, such as data assimilation, and the methods developed here may be useful for those applications. For other applications, however, such as nowcasting and oceanography, it may be relevant to keep the flagged WVCs since their winds provide essential information on (highly variable) air–sea interaction processes that cannot be captured by any other wind observing system. Therefore, using MVD as a verification for QC schemes appears flawed, for many wind applications, since cases with large VD are among the most relevant ones. This sheds new light on existing QC schemes for scatterometer and radiometer winds in general.

Acknowledgment

The authors would like to thank EUMETSAT, for providing the ASCAT level 1b data; the EUMETSAT NWP SAF for developing the software used in this paper; J.-R. Bidlot and ECMWF, for providing the Global Telecommunication System (GTS) buoy wind data set (already quality controlled); and the two reviewers who helped to improve the paper. The ECMWF data were retrieved from the ECMWF Meteorological Archival and Retrieval System (MARS). The TMI data are available from the website of Remote Sensing Systems (http://www.ssmi.com/). The buoy rain data are obtained from http://www.pmel.noaa.gov/.

References

[1] J. Figa and A. Stoffelen, "On the assimilation of Ku-band scatterometer winds for weather analysis and forecasting," *IEEE Trans. Geosci. Remote Sens.*, vol. 38, no. 4, pp. 1893–1902, Jul. 2000.

[2] J. N. Huddleston and B. W. Stiles, "A multi-dimensional histogram technique for flagging rain contamination on QuikSCAT," in *Proc. IEEE Int. Geosci. Remote Sens. Symp.*, Honolulu, HI, USA, 2000, vol. 3, pp. 1232–1234.

[3] M. Portabella and A. Stoffelen, "A comparison of KNMI quality control and JPL rain flag for SeaWinds," *Can. J. Remote Sens.*, vol. 28, no. 3, pp. 424–430, Jan. 2002.

[4] B. W. Stiles and S. H. Yueh, "Impact of rain on spaceborne Ku-band wind scatterometer data," *IEEE Trans. Geosci. Remote Sens.*, vol. 40, no. 9, pp. 1973–1983, Sep. 2002.

[5] K. A. Hilburn, F. J. Wentz, D. K. Smith, and P. D. Ashcroft, "Correcting active scatterometer data for the effects of rain using passive microwave data," *J. Appl. Meteorol. Climatol.*, vol. 45, no. 3, pp. 382–398, Mar. 2006.

[6] D. W. Draper and D. G. Long, "Simultaneous wind and rain retrieval using SeaWinds data," *IEEE Trans. Geosci. Remote Sens.*, vol. 42, no. 7, pp. 1411–1423, Jul. 2004.

[7] C. Nie and D. G. Long, "A C-band scatterometer simultaneous wind/rain retrieval method," *IEEE Trans. Geosci. Remote Sens.*, vol. 46, no. 11, pp. 3618–3632, Nov. 2008.

[8] M. Portabella, A. Stoffelen, A. Verhoef, and J. Verspeek, "A new method for improving scatterometer wind quality control," *IEEE Trans. Geosci. Remote. Sens. Lett.*, vol. 9, no. 4, pp. 579–583, Jul. 2012.

[9] M. Portabella *et al.*, "Rain effects on ASCAT wind retrieval: Towards an improved quality control," *IEEE Trans. Geosci. Remote. Sens.*, vol. 50, no. 7, pp. 2495–2506, Jul. 2012.
[10] A. Turiel, M. Portabella, W. Lin, and J. Ballabrera-Poy, "Quality assessment of ASCAT wind vector maps through singularity analysis," SMOS BEC, Barcelona, Spain, SMOS BEC Tech. Note BEC-TN.2012.02 v.1, Feb. 2012. [Online] Available: www.smos-bec.icm.csic.es/publications
[11] W. Lin, M. Portabella, A. Stoffelen, A. Turiel, and A. Verhoef, "Rain identification in ASCAT winds using singularity analysis," *IEEE Trans. Geosci. Remote. Sens. Lett.*, vol. 11, no. 9, pp. 1519–1523, Sep. 2014.
[12] A. Stoffelen and D. Anderson, "Ambiguity removal and assimilation of scatterometer data," *Q. J. R. Meteorol. Soc.*, vol. 123, no. 538, pp. 491–518, Jan. 1997.
[13] W. Lin, M. Portabella, A. Stoffelen, and A. Verhoef, "On the characteristics of ASCAT wind direction ambiguities," *Atmos. Meas. Tech.*, vol. 6, 1053–1060, 2013.
[14] A. Stoffelen and D. Anderson, "Scatterometer data interpretation: Measurement space and inversion," *J. Atmos. Ocean. Technol.*, vol. 14, no. 6, 1298–1313, Dec. 1997.
[15] A. Verhoef, M. Portabella, A. Stoffelen, and H. Hersbach, "CMOD5.n—the CMOD5 GMF for neutral winds," KNMI, De Bilt, The Netherlands, Ocean Sea Ice SAF Tech. Note SAF/OSI/CDOP/KNMI/TEC/TN/3 165 v.1, May 2008. [Online]. Available: http://www.knmi.nl/publications/fulltexts/cmod5_neutral_winds_1.0.pdf
[16] M. Portabella and A. Stoffelen, "Characterization of residual information for SeaWinds quality control," *IEEE Trans. Geosci. Remote Sens.*, vol. 40, no. 12, pp. 2747–2759, Dec. 2002.
[17] A. Turiel, H. Yahia, and C. Pérez-Vicente, "Microcanonical multifractal formalism: A geometrical approach to multifractal systems. Part I: Singularity analysis," *J. Phys. A*, vol. 41, no. 1, p. 015501, Jan. 2008.
[18] O. Pont, A. Turiel, and C. J. P´rez-Vicente, "Empirical evidences of a common multifractal signature in economic, biological and physical systems," *Phys. A*, vol. 388, no. 10, pp. 2025–2035, May 2009.
[19] O. Pont, A. Turiel, and H. Yahia, "An optimized algorithm for the evaluation of local singularity exponents in digital signals," in *Proc. 14th IWCIA. Lecture Notes in Computer Science*, vol. 6636, J. Aggarwal, R. Barneva, V. Brimkov, K. Koroutchev, and E. Korutcheva, Eds. Berlin, Germany: Springer-Verlag, 2011, pp. 346–357.
[20] C. Anderson, H. Bonekamp, C. Duff, J. Figa-Saldaña, and J. J. W. Wilson, "Analysis of ASCAT ocean backscatter measurement noise," *IEEE Trans. Geosci. Remote. Sens.*, vol. 50, no. 7, pp. 2449–2457, Jul. 2012.
[21] J. Vogelzang, A. Stoffelen, A. Verhoef, and J. Figa-Saldaña, "On the quality of high-resolution scatterometer winds," *J. Geophys. Res.*, vol. 116, no. C10, pp. C10033-1–C10033-14, Oct. 2011.

Wenming Lin was born on April 22, 1984, in China. He received the B.Sc. degree in engineering from Wuhan University, Wuhan, China, in 2006 and the Ph.D. degree in engineering from the Center for Space Science and Applied Research, Chinese Academy of Sciences, Beijing, China, in 2011.

He is currently a Postdoctoral Researcher with the Institut de Ciències del Mar (ICM–CSIC), Barcelona, Spain, working on the scatterometer wind quality control.

Marcos Portabella was born on October 14, 1970 in Spain. He received the B.Sc. degree in Physics in 1994 from the University of Barcelona, Barcelona, Spain; the M.Sc. in Remote Sensing in 1995 from the Institute of Space Studies of Catalonia, Barcelona, Spain; and the Ph.D. degree in Physics in 2002, from the University of Barcelona, Spain.

He is currently with the Institut de Ciéncies del Mar (ICM–CSIC), Barcelona, working on satellite remote sensing. In particular, he is involved in scatterometry and L-band radiometry.

Ad Stoffelen was born on February 25, 1962, in The Netherlands. He received the M.Sc. degree in physics from the Technical University of Eindhoven, Eindhoven, The Netherlands, in 1987 and the Ph.D. degree in meteorology on scatterometry from the University of Utrecht, Utrecht, The Netherlands.

He is currently with the Royal Netherlands Meteorological Institute (KNMI), De Bilt, The Netherlands, and responsible for the ASCAT wind products. He is also deeply involved in the European Space Agency Atmospheric Dynamics Mission (ADM)-Aeolus Doppler Wind Lidar Mission.

Anton Verhoef was born on December 10, 1964, in The Netherlands. He received the M.Sc. degree in physics and the Ph.D. degree in solid state physics from the Rijksuniversiteit Groningen, Groningen, The Netherlands, in 1989 and 1994, respectively.

He is currently with the Royal Netherlands Meteorological Institute (KNMI), De Bilt, The Netherlands, working on scatterometry processing software development, data validation, quality monitoring, and user services.

Antonio Turiel was born on May 1, 1970, in Spain. He received the B.Sc. degree in physics, the B.Sc. degree in mathematics, and the Ph.D. degree in theoretical physics from the Autonomous University of Madrid, Madrid, Spain, in 1993, 1994, and 1998, respectively.

He is currently with the Department of Physical Oceanography, Institut de Ciències del Mar (ICM–CSIC), Barcelona. His research topics include signal and image processing applied to remote sensing of the oceans, marine turbulence at mesoscale, and ocean circulation at different scales.